International Journal of Fluid Power 4 (2003) No. 2 pp. 15-24

THREE-DIMENSIONAL ANALYSIS OF FLOW FORCES ON DIRECTIONAL CONTROL VALVES

Giuseppe Del Vescovo and Antonio Lippolis

Dipartimento di Ingegneria Meccanica e Gestionale, Politecnico di Bari, Via Re David 200, 70125 Bari, Italy
g.delvescovo@poliba.it, lippolis@poliba.it

Abstract

This paper deals with a sufficiently complete analysis of flow forces acting on spools of hydraulic directional control valves. The analysis performed, using the very reliable and commercially widespread "Fluent" code, aims to describe global parameters in order to evaluate such forces with a reasonable accuracy and without performing expensive three-dimensional calculations. To this aim, different fluid dynamics analyses have been carried out inside the valve, starting from simple axis-symmetric models, up to full three-dimensional simulations. A comparison of the 2D and 3D results is then presented.

Keywords: CFD simulation, flow forces, directional valves

1 Introduction

One of the fundamental issues to be considered for a good design of a directional valve is the prediction of flow forces acting on the spool. These forces tend to close the spool immediately after the first phase of opening; the driving system should be able to overcome these forces if a fast opening of the valve is desired.

The considered plant is shown in Fig. 1: the pump delivers a constant flow rate to the pressure relief valve (3) and to the directional valve (4). In the first opening phase the flow rate to the user line is small, and the pressure is substantially constant and equal to the pressure imposed by the open relief valve. The fluid dynamic force acting on the spool grows approximately linearly with its opening. Subsequently the flow rate across the directional valve reaches the pump flow rate. Therefore, it remains constant while the pressure drop between the upstream and downstream valve positions decreases. In this phase, the pressure relief valve is closed; the force acting on the spool is subject to two contrasting phenomena: the growth of the opening and the diminishing of the pressure drop. The latter is prevailing, and consequently the flow force acting on the spool decreases. In order to open and close the valve quickly, the spool driving system must be able to overcome the reached maximal force; according to these considerations, the dynamic limit of the valve is determined by the greatest allowable pump flow rate.

This manuscript was received on 28 Januar 2003 and was accepted after revision for publication on 25 June 2003

The present paper presents a sufficiently complete analysis of the flow conditions that, in the phase of opening, determine the dynamic limit of the valve.

The analysis has been performed by means of “Fluent” code. Results are based on the numerical segregated solution of Reynolds averaged Navier Stokes equations for incompressible flows including transport equations of turbulence quantities K and ε.

The fluid dynamic analysis of each case has been preceded by the creation of opportune computational grid by means of *PREBFC* or Gambit pre-processor software: grids used in all the cases are block structured; in some of the three-dimensional analyses, computational grid has been obtained by means of the rotation of the previously realized two-dimensional one.

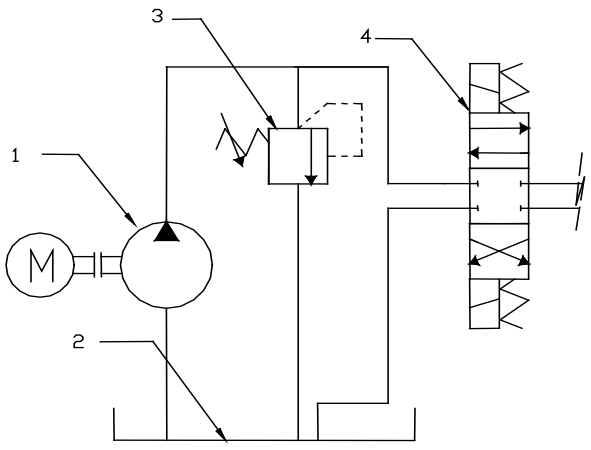

Fig. 1: *Reference hydraulic system*

At any rate, boundary conditions are:

- total pressure and direction of the flow in the INLET section,
- static pressure in the OUTLET section.

The turbulence model used is the so-called "Two-Layer Zonal Model", that solves differently two zones of flow: near the walls it uses damping functions for the determination of turbulence characteristic length and solves only the transport equation for kinetic turbulent energy *K*, while in the central flow zone it uses the classical turbulence model *RNG K-ε*, that is the most reliable model for separated flows strongly influenced by recirculation zones.

The study could be considered sufficiently exhaustive because both axis-symmetric and three-dimensional analyses have been carried out.

In order to test physical validity of numerical results a detailed analysis of the grid influence has been realized in a previous work (Del Vescovo and Lippolis, 2002) on a 3D model of a four-way valve. The last analysis has shown a great reliability of Fluent code in this type of applications because the computed global results (i.e. flow rate and flow forces) are sensibly grid independent.

The three-dimensional modelling aims to identify the causes of the disagreement between simplified axis-symmetric numerical results and experimental tests on directional control valves (Borghi et al, 2000).

2 Axis-symmetric Analysis

The hypothesis of axis-symmetric flow simplifies considerably the memory and CPU request necessary to the CFD analysis. Therefore, with the same computational resources, the axis-symmetric analysis allows to use very fine computational grids, adequate to a detailed study of turbulence effects.

Unfortunately, the geometry of the valve is not axis-symmetric because *P*, *A*, *B* and *T* port connections are located in a precise angular position, while the remaining parts of the chambers are limited by the body valve walls (refer to Fig. 2).

In the present paper, the axis-symmetric analysis aims to be only a reference model in order to evaluate the approximations that this model produces.

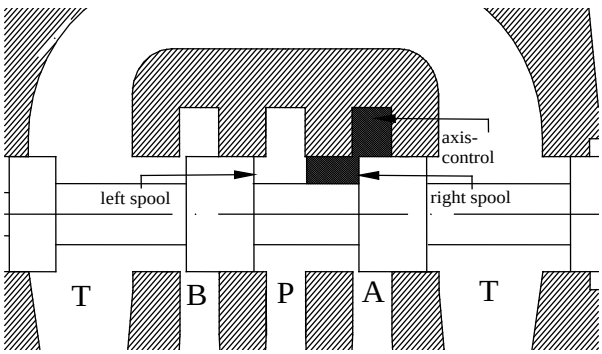

Fig. 2: *Valve geometry and axis-symmetric control volume*

Figure 2 shows the simplified axis-symmetric reference geometry and puts in evidence the control volume modelled and meshed by pre-processor software. Total pressure value and inlet axial flow direction have been enforced as boundary condition on a section of the annular channel that connects *P* to the metering section while the outlet static pressure has been imposed on the external surface of the discharge cylindrical chamber.

In the axis-symmetric model the two aforementioned sections coincide respectively with the lower-left vertical segment and the upper-right horizontal segment as shown in Fig. 4.

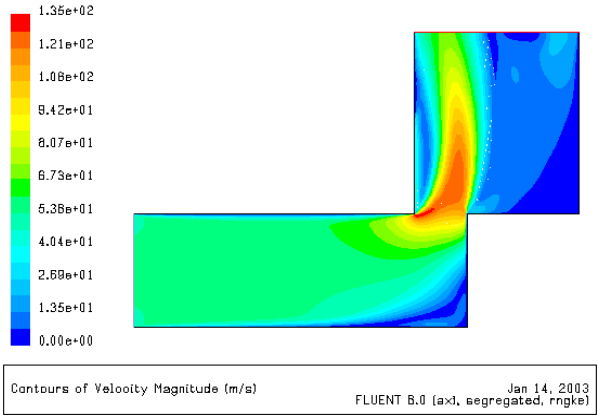

Fig. 3: *Velocity contours, axis-symmetric example*

Figures 3 and 4 show the obtained numerical results for about 0.13 ratio between spool opening and spool external diameter (*x*/*D*). Figure 3 shows the velocity contours: a slow and gradual acceleration of the fluid could be noticed at first; the acceleration becomes very abrupt near the restricted section where the flow turns its pressure energy into kinetic energy. Only the lower-right corner of axial channel is characterized by stagnating fluid that does not give an appreciable contribution to the general flow. Beyond the restricted section, there are two distinguishable zones: a very rapid central flow and a surrounding zone characterized by very low oil velocity.

The great shear forces between the two zones produce a gradual deceleration of the flow core, without any appreciable pressure recovery.

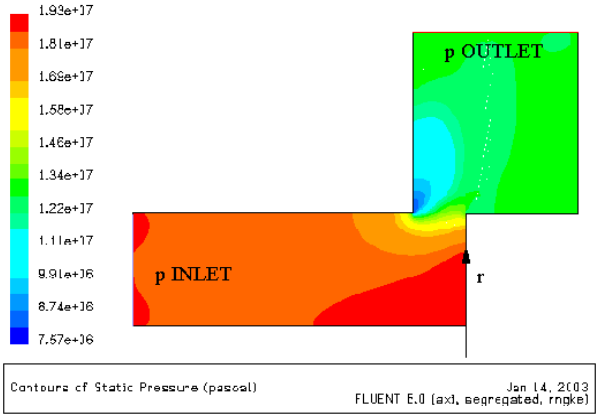

Fig. 4: *Pressure contours, axis-symmetric example*

The same analysis could be realized with reference to the Fig. 4 that shows the static pressure contours. The separation of pressure values between the two domains upstream and downstream of the metering section is evident. This phenomenon is due to the abrupt decrease of

static pressure close to the metering section. Moreover, downstream of the restricted section, the pressure is approximately constant, without any substantial recovery due to the flow deceleration. Indeed, this zone is essentially characterized by the dissipation of the mean flow kinetic energy by means of turbulence effects that take place in the lateral zones of the central high velocity flow (Del Vescovo and Lippolis, 2002); downstream of the metering section, a recirculation bubble determines a low-pressure stagnating zone.

The static pressure profile on the prominence of the spool is at the origin of the axial force acting on the spool and is represented in graphic form in Fig. 5 where it can be noticed the decrease of the relative pressure value defined as:

$$p_{\text{rel}} = \frac{p - p_{\text{outlet}}}{\Delta p} \tag{1}$$

with the non-dimensional radial distance, defined as the ratio between the distance from the axis and the spool diameter D (refer to the Fig. 4), i.e.:

$$r^* = \frac{r}{D} \tag{2}$$

In fact, the axial flow force has been evaluated integrating the static pressure field, provided by the numerical solution, on the right spool face and stating that the pressure acting on the left spool face is constant and equal to the INLET total pressure (refer to the Fig. 2).

Other details of the flow inside the valve at other opening values, extremely interesting from a fluid dynamics point of view, are neglected because they are beyond the aims of the present paper. It is worth showing the influence of pressure drop on global parameters, i.e. flow rate and flow force.

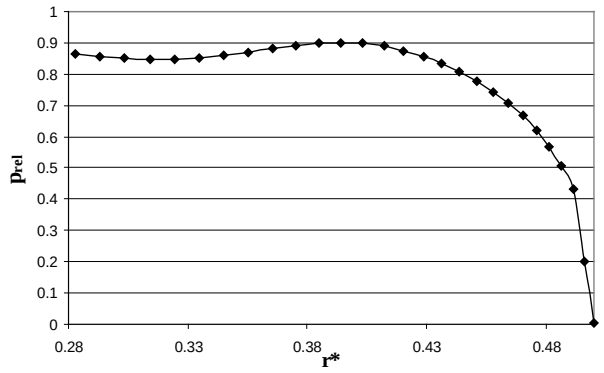

Fig. 5: *Static pressure on spool face*

In order to give a general validity to the performed results the following two non-dimensional parameters have been used:

$$C_{\text{d}} = \frac{Q}{\pi D x \sqrt{\frac{2\Delta p}{\rho}}} \tag{3}$$

$$K = \frac{F_{\text{spool}}}{\frac{\pi(D^2 - d^2)}{4}\Delta p} \tag{4}$$

where Q is the flow rate, ρ the density of the fluid, D and d are, respectively, the external and internal diameter of the prominence of the spool, x is the spool axial travel from the rest position, that coincides with the opening of the valve, F_{spool} is the axial flow force acting on the spool and Δp is the enforced pressure drop.

The first parameter is the classical definition of the discharge coefficient. It represents the ratio between the actual mass flow rate and the theoretical one calculated considering a uniform velocity profile in the restricted geometric section and, considering that, according with the classical Borda hypothesis, all the pressure energy turns into kinetic energy up to the metering section without any subsequent pressure recovery.

The K parameter is the non-dimensional flow force and represents the average static pressure value that, acting on a single spool face, creates an axial force equal to the flow force; it is expressed proportionately to the enforced pressure drop.

Figure 6 shows the dependence of the previously mentioned two coefficients on the pressure drop: it could be noticed that there is an almost perfect constancy of the discharge coefficient and of K parameter with the pressure drop thus confirming the predominance of localized pressure losses; only at the lower Δp there is an increase of two coefficients.

The discharge coefficient values are influenced by two different phenomena that could be noticed in the velocity contours (Fig. 3): velocity in the turbulent core respects, with good approximation, the Borda hypothesis, but the fluid dynamics restricted section (i.e. *vena contracta area*) is smaller than the geometric one, while the presence of boundary layers reduces the average velocity, particularly at very little openings.

The value of the discharge coefficient is approximately 0.6 and this is the typical value pertaining to other fluid dynamic phenomena, e.g. internal combustion engine valves and diaphragms for flow rate measurements.

K value is approximately 0.2 and shows that the axial force on the spool cannot be neglected.

In the same diagram there are two other non-dimensional parameters defined as below:

$$\text{Re} = \frac{2x\sqrt{2\rho\Delta p}}{\mu} \tag{5}$$

$$\beta = \frac{K}{C_{\text{d}}^2} = \frac{8\pi\ x^2}{\rho\left[1 - \left(\frac{d}{D}\right)^2\right]}\frac{F_{\text{spool}}}{Q^2} \tag{6}$$

where the first is the classical Reynolds number and is defined considering the theoretical velocity (according to the Borda hypothesis) and the equivalent hydraulic diameter of the circumferential metering section. The values of Reynolds number vary between 2000 and 12000.

The latter is a new parameter proposed by the authors for the valve design: this parameter, which is the combination of the other two non-dimensional parameters, connects directly flow force and flow rate, removing the dependence on the pressure drop.

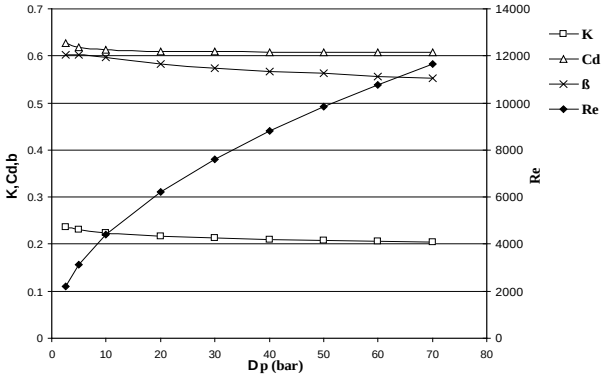

Fig. 6: *Parameters at different pressure drops*

In fact, while the axial force and the flow rate are easily identifiable, the pressure drop is more difficult to define. It must be noticed that in the definition of C_d and K, the pressure drop between upstream and downstream of the metering edge should be rigorously considered while the value that is actually used in Eq. 3 and 4 is the pressure drop on the whole computational domain between INLET and OUTLET sections. The difference between the two values is due to the pressure losses upstream and downstream of metering section and decreases the physical meaning of computed K and C_d parameters.

This observation will be of remarkable importance in the three dimensional models.

Figure 7 shows the variations of these parameters versus the valve opening; the decrease of the C_d value at the greatest openings is due to the increasing pressure losses far from the metering section. These pressure losses reduce the actual pressure drop and, consequently the velocity in the metering section, decreasing the flow rate and, apparently, the discharge coefficient C_d.

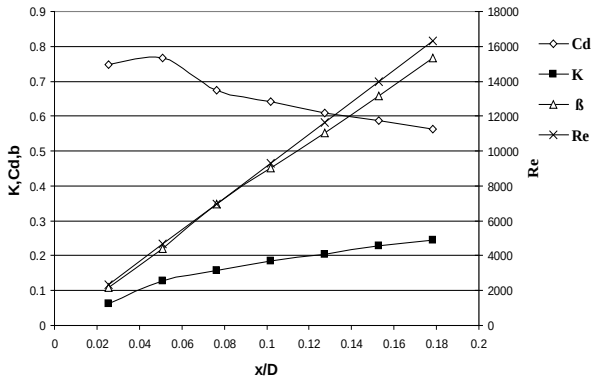

Fig. 7: *Parameters at different spool openings*

The decrease of the C_d value at the smallest openings puts in evidence the strong influence of boundary layer effects at the smallest spool openings.

The same analysis concerns the K parameter that increases less linearly because of the reduction of pressure drop on the metering section.

β coefficient profile is practically linear with the valve opening thus confirming its validity. This property, due to the independence on pressure drop, makes it very interesting.

Reynolds number, which, by definition is proportional to the opening, varies between 2000 and 16000.

3 Outlet Flow Three-dimensional Analysis

Existing papers in literature (Borghi et al, 2000; Macor et al, 1999) deal only with two-dimensional analysis, similar to that performed in the previous section, because the generation of the computational grid is simpler and requires a limited computational effort.

One of the aims of the present paper is to verify if a two-dimensional approximation is acceptable. Indeed, the port connections eliminate the perfect axis-symmetry of the valve. In this paragraph, the actual 3D OUTLET section geometry is being considered, while the INLET section geometry is still being assumed axis-symmetric.

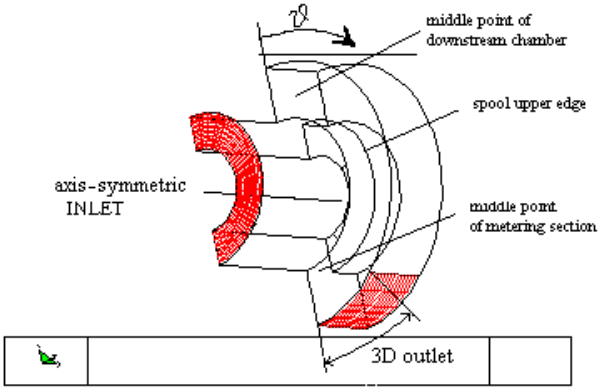

Fig. 8: *3D geometry with axis-symmetric INLET*

Figure 8 shows the computational domain and puts in evidence the grids on the two aforementioned INLET and OUTLET sections.

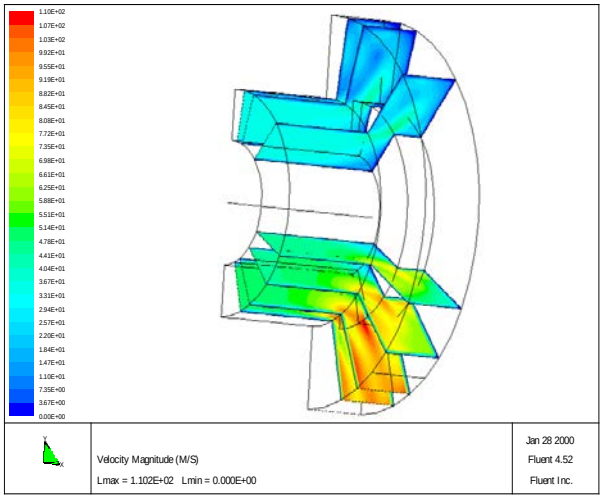

Fig. 9: *Velocity contours on meridian planes*

Exploiting the symmetry of the problem only half a valve has been modeled and, in order to simplify the grid generation, a rectangular OUTLET section has been adopted instead of the more realistic circular one. Figures 9 and 10 show velocity and pressure contours on a series of meridian planes that provide a sufficiently complete image of the three-dimensional field.

For each meridian plane, contours are qualitatively similar to those performed by the axis-symmetric model: the flow accelerates abruptly in correspondence of

the metering section determining a high velocity flow in the downstream chamber while pressure values are separated by the restricted section. From a quantitative point of view, it must be underlined a considerable difference between the meridian planes: planes that are in proximity of the outflow duct are interested by a more intense flow than upper planes that present a lower pressure drop on the metering section. In fact, the circumferential flow directed towards the outlet section produces not negligible circumferential pressure losses.

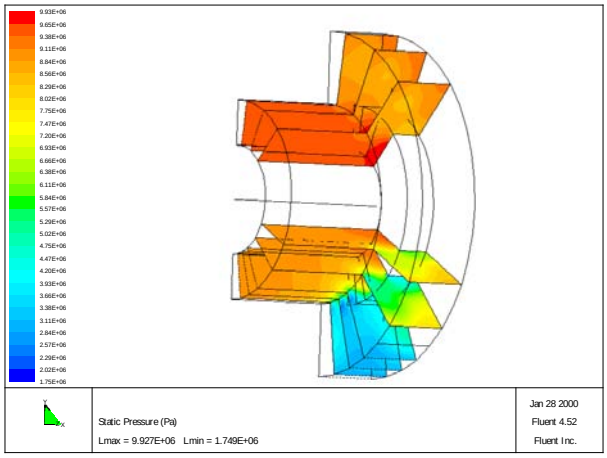

Fig. 10: *Static pressure contours on meridian planes*

To better show the approximations created by an axis-symmetric analysis, Fig. 11 presents the overlapped profiles of the static pressure in the two models on the upper edge of spool prominence ($r^* = 0.5$) at the different angular position ϑ, as indicated in Fig. 8.

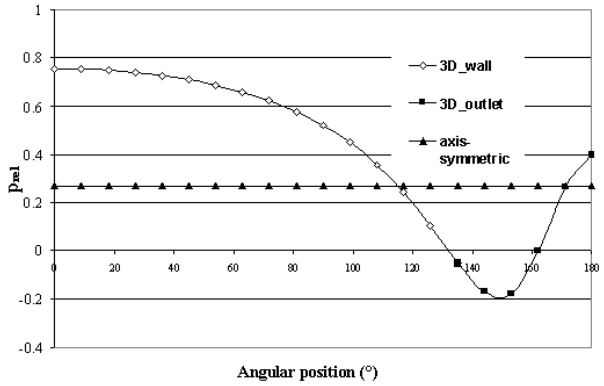

Fig. 11: *Pressure on spool edge*

The profile relative to three-dimensional model is divided into two parts, the first facing the body valve wall (3D_wall), the latter facing the outlet section (3D_outlet) as shown in Fig. 8.

It can be noticed that the constant value of the axis-symmetric simulation is very far from three-dimensional results that present a pressure value that decreases, reaches a minimum in correspondence of the outlet section and subsequently increases up to the symmetry plane.

The latter phenomenon is explainable pointing out that in the downstream chamber there are two counter-rotating circumferential flows carrying a flow rate corresponding to 180 degrees of the valve; on the symmetry plane the tangential velocity component vanishes, thus determining a static pressure recovery.

A decreasing distribution of pressures on the face of the spool determines, obviously, a not centered position of the elementary forces resultant.

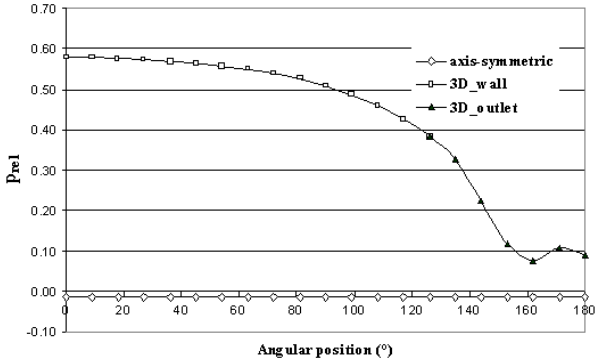

Fig. 12: *Pressure in the middle of downstream chamber*

Figure 12 shows the value of static pressure in the middle point of downstream chamber as indicated in Fig. 8. It can be noticed that the axis-symmetric model underestimates the whole pressure profile because it does not consider circumferential pressure losses and consequently overestimates velocities in the metering section as shown in Fig. 13.

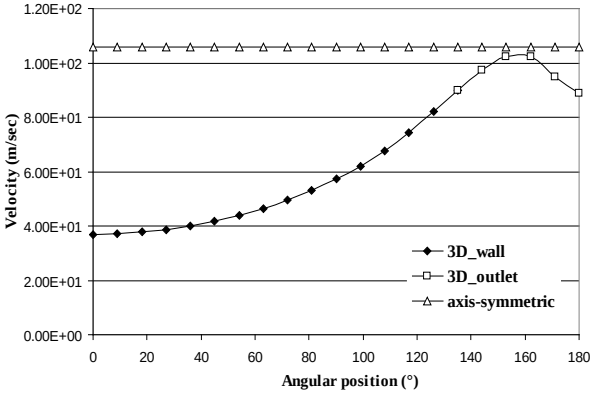

Fig. 13: *Velocity magnitude in the metering section*

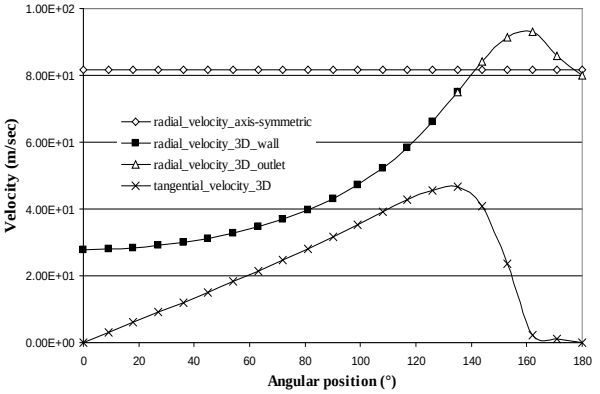

Fig. 14: *Radial and tangential velocity in the metering section*

Velocity values, presented in Fig. 13 refer to the velocity magnitude, while Fig. 14 shows radial and tangential components in the metering section: three-dimensional model presents, in correspondence of out-

flow section, a radial velocity value greater than the axis-symmetric model one, and this is due to the circumferential flow in the downstream chamber that reduces the axial component and increases the corresponding radial one.

The diagram of Fig. 14 plots also the circumferential velocity. It shows an almost linear increase of tangential component from the symmetry plane up to a section that is near the outflow section. Subsequently there is a decrease of the tangential components up to the symmetry plane where it, obviously, vanishes.

4 Full Three-dimensional Analysis

Finally, a full three-dimensional analysis has been performed, removing the approximation of axis-symmetric INLET flow. In fact, the valve shows a central chamber in which the high-pressure oil is introduced. This central chamber is connected to the high-pressure port in a precise circumferential position.

The general geometry in the physical domain is presented in Fig. 15 where the INLET and OUTLET sections have been underlined in blue, while the symmetry plane is represented in yellow.

In this case, the whole valve geometry can be modeled with the possibility to analyze pressure distribution on both spool prominences (green walls in Fig. 15)

Simulations for different openings have been performed using a so-called “deforming mesh” that allows to define the spool travel and to analyze all the openings with only one predefined computational grid.

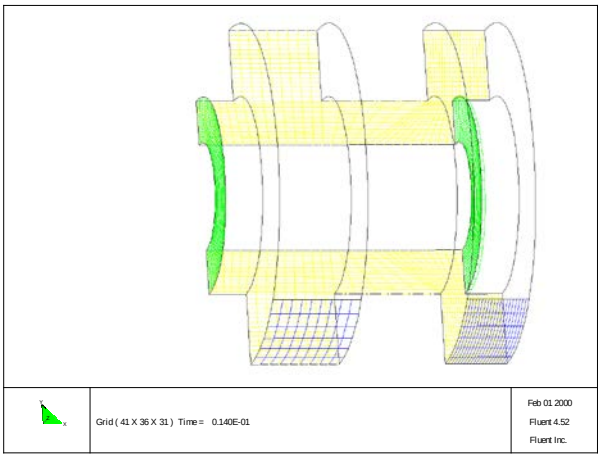

Fig. 15: *Full three-dimensional valve geometry*

Obviously, the same axial velocity to simulate the rigid movement of the spool in axial direction has been imposed for the two corresponding surfaces of spool prominences.

The presence of the left prominence allows a rigorous calculation of the axial force acting on the spool while in the previous models the hypothesis of constant pressure, evaluated as equal to the INLET total pressure, is necessary. The last assumption is a reasonable but not rigorous approximation.

Figure 16 shows iso-velocity and iso-static pressure curves on a series of meridian planes for about 0.13 *x*/*D* ratio.

In this case, differences between planes are increased by the presence of pressure losses in the central chamber, that had not been considered in the previous simplified three-dimensional model.

Figure 17 presents a situation of a very small valve opening value (*x*/*D* equal to 0.013). The Coanda effect that appears in the axis-symmetric simulations (not here reported for brevity of exposure) is evident in the three-dimensional model too, but this phenomenon is reduced.

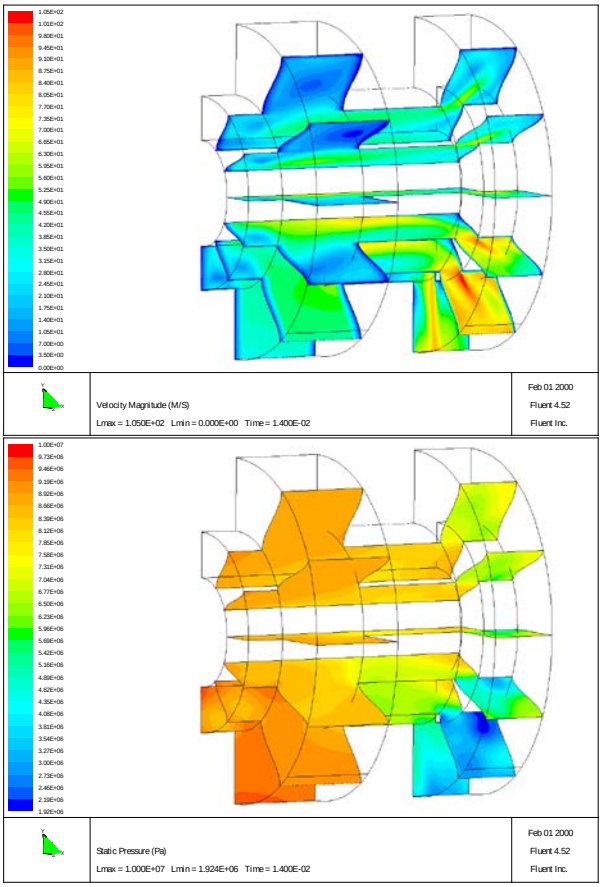

Fig. 16: *Velocity and pressure contours, x/D=0.13*

In fact, a compared qualitative analysis between the two models shows that the Coanda effect disappears in the three-dimensional model at a valve opening value smaller than the axis-symmetric model one.

It must be underlined that the low flow rate that characterizes this small valve opening produces low circumferential pressure losses and consequently a good axis-symmetry of the flow.

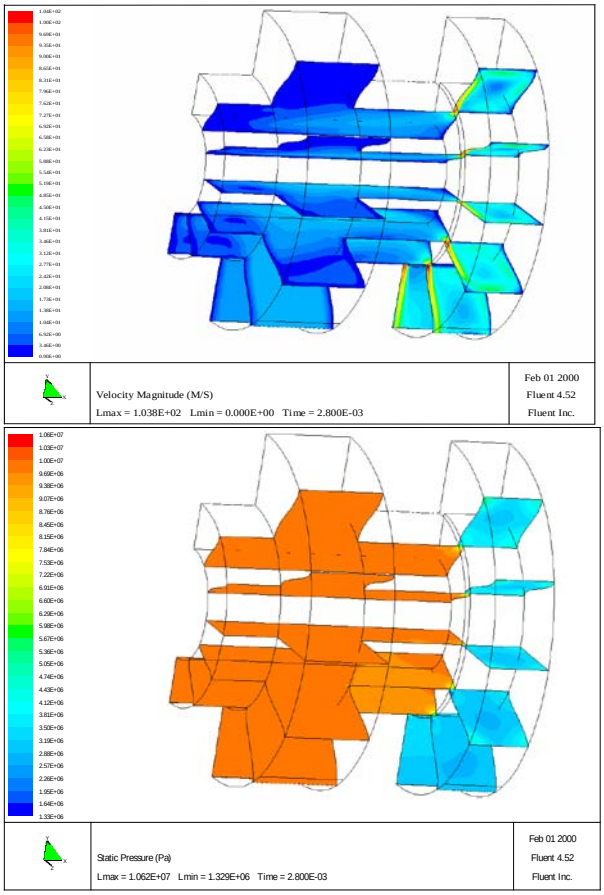

Fig.17: *Velocity and pressure contours, x/D=0.013*

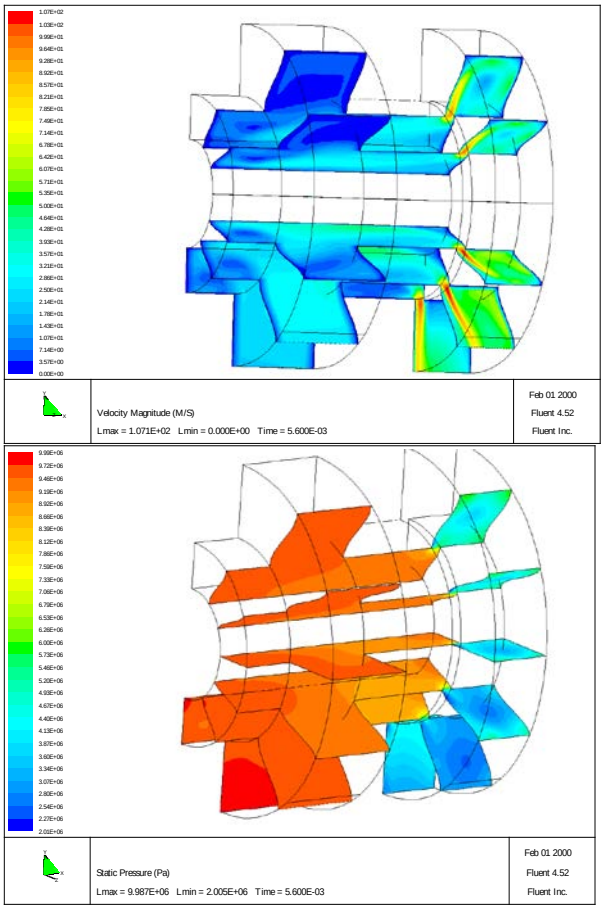

Fig. 18: *Velocity and pressure contours, x/D=0.05*

This observation is confirmed by the uniform distribution of pressure values upstream and downstream of the metering section, with pressure losses concentrated almost completely on it.

In order to complete the analysis, Fig. 18 presents the solution relative to a middle valve opening: it could be noticed that the efflux determines, in many angular positions, the separation of the flow from vertical wall thus decreasing the Coanda effect.

Pressure profiles on the different meridian planes become different because of the growth of circumferential flows in both chambers.

In order to underline these qualitative observations, the following diagrams present the dependence of velocity and pressure on angular position at five different valve openings *x/D* (from 0.013 up to 0.13): the plot of Fig. 19 refers to the pressure on the upper edge of the spool prominence ($r^* = 0.5$) for different valve openings.

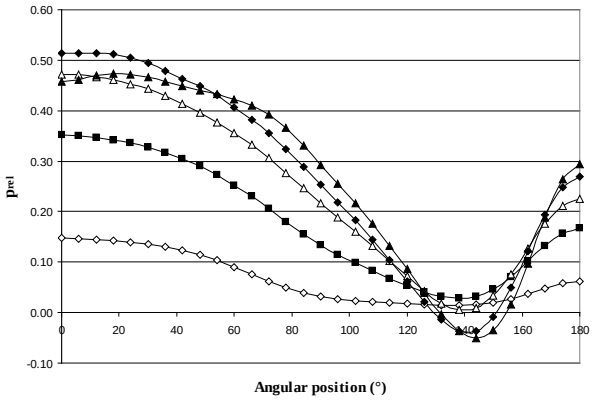

Fig. 19: *Pressure on spool edge at different openings*

In the upper circumferential position, pressures are growing with the valve opening because of the increasing importance of pressure circumferential losses that grow with the increasing flow rate. Figure 20 shows the velocity profiles in the middle point of restricted section and confirms the almost perfect axis-symmetric flow field at small openings and the progressive differentiation.

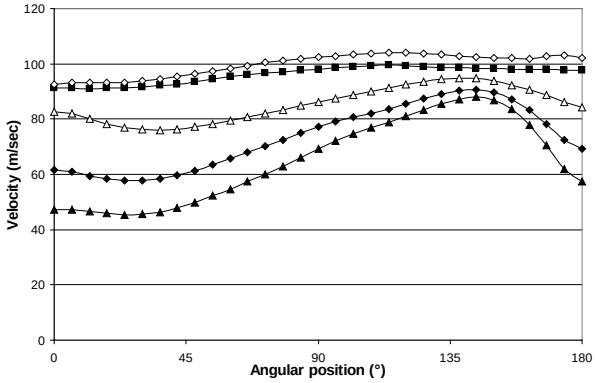

Fig. 20: *Velocity in the metering section at different openings*

5 Compared Numerical Results

Results obtained with three-dimensional models have been analyzed by means of non-dimensional coefficients to better compare the different models.

Figure 21 shows the discharge coefficient profiles; the independence of the discharge coefficient on the pressure drop is confirmed but, as easily predictable, the three-dimensional models provide discharge coefficient values that are about 30% lower than the axis-symmetric model ones.

In fact, pressure circumferential losses reduce the pressure drop on the metering edge and consequently reduce the flow rate.

Figure 22 shows the different profiles of the *K* coefficient; values obtained with an axis-symmetric simulation are greater than the same values provided by three-dimensional models.

The diagram shows a not particularly evident difference between the results obtained with the two three-dimensional models, but it must be considered that only the full three-dimensional model provides rigorously the axial force acting on the left spool face.

Therefore, in the same figure, there is another non-dimensional parameter:

$$K_{\text{left}} = \frac{F_{\text{th}} - F_{\text{left\_full\_3d}}}{\frac{\pi(D^2 - d^2)}{4}\Delta p} \tag{7}$$

where F_{th} is the theoretical force acting on the left spool, i.e.:

$$F_{\text{th}} = \frac{\pi(D^2 - d^2)}{4} p_{\text{inlet}} \tag{8}$$

while $F_{\text{left\_full\_3D}}$ is the force acting on the left spool prominence deriving from the numerical integration of static pressure field computed by Fluent.

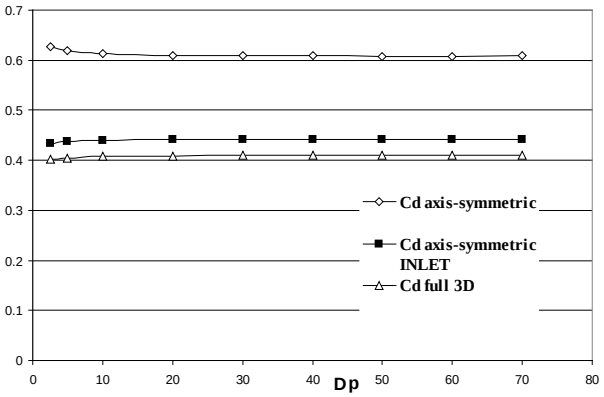

Fig. 21: *Discharge coefficient at different pressure drop in the three models*

The distribution of K_{left} in Fig. 22 shows an approximately constant value equal to 0.15, pointing out that the average pressure on spool left prominence is different from the enforced INLET pressure. Moreover, the full three-dimensional model provides a coexistent remarkable reduction of the average pressure on the right prominence too.

The combination of these two reductions determines a 20% increase of the flow force with respect to the value provided by the axis-symmetric INLET model.

Analysis of the effects owed to the valve opening leads to similar conclusions; Fig. 23 shows that the discharge coefficient presents a notable mismatch between the axis-symmetric and three-dimensional models. This difference grows with the valve opening because of the growing importance of circumferential pressure losses due to the increasing flow rate.

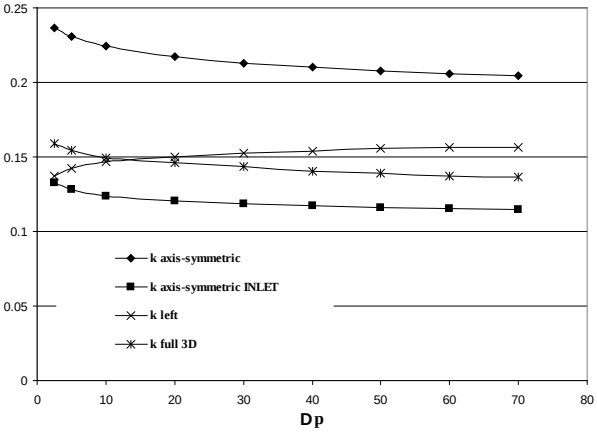

Fig. 22: *K coefficients at different pressure drop in the three models*

In the Fig. 23 the variation of *K* coefficients with the valve opening for the different models is shown; the differences grow at the greatest openings also in this case.

β coefficient profiles are shown in Fig. 24. This coefficient can be considered the most non-dimensional reliable coefficient because its profile is approximately linear with the valve opening. The last property is due to its independence on the pressure losses far from metering section.

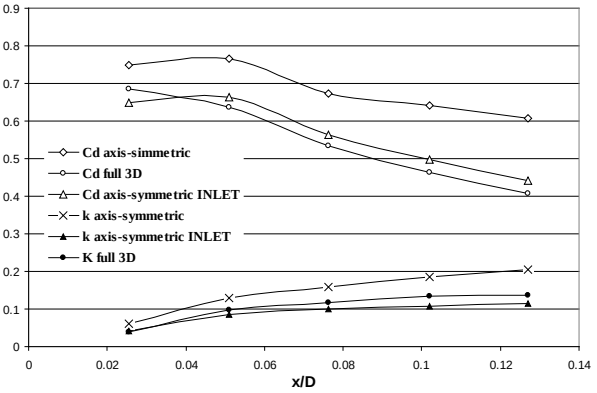

Fig. 23: *K and C_d coefficients at different openings in the three models*

In fact, pressure drop value, considered in the computation of C_{d} and *K* parameters, is different from pressure drop in the metering section; this problem, underlined in the section 2, becomes evident in the three dimensional models where the importance of pressure losses far from metering edge grows and, above all, pressure drop in the metering circumferential section is a function of angular position.

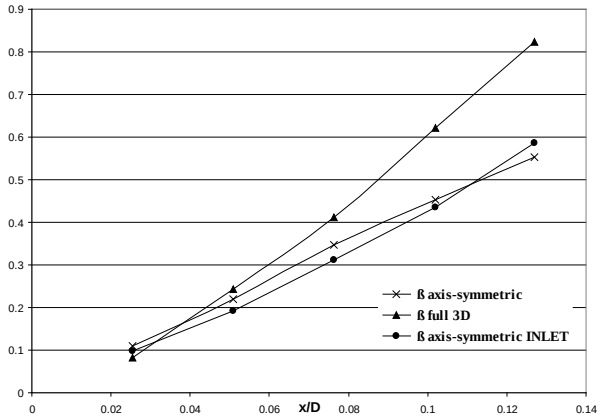

Fig. 24: *β coefficients at different openings in the three models*

The goal of the β parameter introduction has been to calculate its value by a simplified simulation model, (e.g. axis-symmetric), and then to consider it valid also for the three-dimensional case. The last diagram shows that the hypothesis is valid only at the smallest openings; at the greatest openings, there is a coincidence between the axis-symmetric and axis-symmetric INLET model, while the complete three-dimensional model presents different values pointing out that β values, provided by the simplified models, must be opportunely increased.

6 Conclusions

A sufficiently complete analysis of flow conditions in hydraulic directional control valves has been presented. The results of the numerical simulations performed with Fluent, confirm experimental previous results (Borghi et al, 2000; Macor et al, 1999) and point out that the flow rate is proportional to the square root of pressure drop.

Moreover, the three-dimensional analysis points out that the circumferential flows and the consequent pressure losses are not negligible so that the computation of the flow rate and of flow axial force by means of a purely axis-symmetric model determines an unacceptable global parameters estimation.

In the present paper, a new non-dimensional coefficient that connects directly the flow force to the flow rate has been proposed.

This coefficient, evaluated by means of an axis-symmetric analysis, can be used only for small opening values.

Future researches will analyze, numerically and experimentally, complex geometries.

Furthermore, more detailed studies of the influence of the turbulence model on numerical results will be performed.

Nomenclature

ρ	fluid density	[kg/m³]
K	flow force parameter	[-]
μ	dynamic viscosity	[Pas]
ε	turbulent dissipation rate	[-]
C_d	discharge coefficient	[-]
Δp	pressure drop	[Pa]
K	flow force coefficient	[-]
D	spool external diameter	[m]
d	spool internal diameter	[m]
r	radial distance from spool axis	[m]
p_{inlet}	enforced inlet total pressure	[Pa]
p_{outlet}	enforced outlet static pressure	[Pa]
p_{rel}	non-dimensional static pressure	[-]
x	spool axial travel	[m]
F_{spool}	flow force on spool	[N]
K_{left}	left force parameter	[-]
F_{th}	theoretical force on left spool prominence	[N]
β	flow force / flow rate parameter	[-]

References

Batoli, M. 1996. Analisi teorico-sperimentale delle forze di flusso in un distributore a comando elettrico. *Oleodinamica e Pneumatica*.

Borghi, M., Milani, M. and **Paoluzzi, R.** 2000. Stationary axial flow force analysis on compensated spool valves. *International Journal of Fluid Power*, Vol. 1, No. 1, pp. 17-25.

Fluent Inc. 1995. *Fluent Europe user's guide*, Vol. 1-4.

Fluent Inc. 1995. *Fluent tutorial guide*, Vol. 1, 2.

Fluent Inc. 2000. *Gambit user's guide.*

Fluent Inc. 2000. *Gambit Modeling guide.*

Macor, A. and **Badin, D.** 1999. Influenza dei modelli di turbolenza nello studio delle forze di flusso nei distributori oleoidraulici. *Proceedings of 54° Congresso Nazionale ATI*, L'Aquila.

Macor A. and **Dato, S.** 2000. La riduzione delle forze di flusso in un distributore oleoidraulico mediante sagomatura della sezione ristretta. *Proceedings of 55° Congresso nazionale ATI*, Bari-Matera.

Macor A. 2002. Analisi sperimentale di un distributore oleodinamico con sezione ristretta a intaglio piano. *Proccedings of 57° Congresso Nazionale ATI*, Pisa.

Nervegna, N. 2000. Componenti - Vol. 2. *Oleodinamica e Pneumatica*, Torino: Politeko.

Speich, H. and **Bucciarelli, A.** 1976. *L'Oleodinamica.* Tecniche Nuove, Milano.

Del Vescovo, G. and **Lippolis, A.** 2001. Analisi delle forze diflusso in un distributore a comando elettrico. *Proceedings of the III International Congress MiniHydro*, Maratea.

Del Vescovo, G. and **Lippolis, A.** 2002. Flow forces analysis on a four way valve. *Proceedings of 2nd FPNI PhD Symposium*, Modena, Italy.

Wilcox, D. C. 1998. *Turbulence Modeling for CFD.*

Wu, D., Burton, R. and **Schoenau G.** 2002. An empirical discharge coefficient model for orifice flow. *International Journal of Fluid Power*, Vol. 3, No. 3, pp. 13-17.

Giuseppe Del Vescovo
Born in Bari (BA) in 1975. Graduated in Mechanical Engineering (2000) at the Politecnico di Bari, Italy. Since January 2001, he is Fluid Power PhD Student at the Politecnico di Bari. His research interests are focused on the application of CFD in the analysis of flows in hydraulic valves.

Antonio Lippolis
Born in Gioia del Colle (BA) in 1955. Graduated in Mechanical Engineering (1981) at the Politecnico di Bari (Italy). Researcher at the Faculty of Engineering of the Politecnico di Bari since 1983, at present he is Professor in Fluid Power Systems. Author and co-author of more than 40 papers dealing with "Numerical Fluid-Dynamics" and "Fluid Power".